

Advanced Multilayer Amorphous Silicon Thin-Film Transistor Structure: Film Thickness Effect on Its Electrical Performance and Contact Resistance

Alex KUO, Tae Kyung WON¹, and Jerzy KANICKI*

Organic and Molecular Electronic Laboratory, Department of Electrical Engineering and Computer Science, University of Michigan, Ann Arbor, MI 48109, U.S.A.

¹*Applied Komatsu Technology America Inc., Santa Clara, CA 95054, U.S.A.*

(Received December 4, 2007; accepted February 4, 2008; published online May 16, 2008)

We report the intrinsic and extrinsic electrical characteristics of advanced multilayer amorphous silicon (a-Si:H) thin-film transistor (TFT) with dual amorphous silicon nitride (a-SiN_x:H) and a-Si:H layers. The thickness effect of the high electronic quality a-Si:H film on the transistor's electrical property was investigated; with increasing film thickness, both field-effect mobility and subthreshold swing show improvement and the threshold voltage remain unchanged. However, the contact resistance increases with the a-Si:H film thickness. Using the two-step plasma enhanced chemical vapor deposition process, we fabricated TFT's with acceptable field-effect mobility ($\sim 1 \text{ cm}^2 \text{ V}^{-1} \text{ s}^{-1}$) and threshold voltage ($< 1.5 \text{ V}$) with enhanced throughput. [DOI: [10.1143/JJAP.47.3362](https://doi.org/10.1143/JJAP.47.3362)]

KEYWORDS: amorphous silicon thin-film transistor, dual layer, thickness effect, contact resistance

1. Introduction

As the active-matrix liquid crystal display (AM-LCD) industry begins to introduce large-size and high-pixel-density displays, the demand for a high performance amorphous silicon thin-film transistor mounts. In order for the hydrogenated amorphous silicon (a-Si:H) thin-film transistor (TFT) to remain competitive in the flat-panel display industry, it is necessary to realize transistors with a high field-effect mobility and a low threshold voltage while being able to be fabricated at a high deposition rate.¹⁾ These qualities allow the possibility of manufacturing large displays with low power consumption at relatively low costs. Fabricating high performance a-Si:H TFT requires a high electronic quality a-Si:H film, as the electrical characteristics of a TFT is intimately related the electronic quality of the a-Si:H film.²⁾ Even though a high electronic quality film can be achieved by lowering its plasma-enhanced chemical vapor deposition (PECVD) rate, doing so increases the overall device fabrication time. In the AM-LCD industry, the inverted staggered back-channel-etched type transistor structure is preferred over the tri-layer type transistor structure because of its reduced photolithography steps and improved source/drain contact quality.³⁾ This structure requires the deposition of a thicker amorphous silicon film for better control of the back channel etch step.⁴⁾ However, a thicker amorphous silicon film for TFT means longer deposition time, which also leads to a lower production output and higher overall costs for the AM-LCD industry.⁵⁾ The PECVD time can be shortened by increasing the deposition rate of the film, but doing so degrades the mobility and threshold voltage of the transistor.⁶⁾ Similarly, the gate insulator amorphous silicon nitride (a-SiN_x:H) should exceed 4000 Å to reduce the gate leakage. Also its PECVD rate needs to be low in order for the a-Si:H TFT to have a high electronic quality a-SiN_x:H/a-Si:H interface for optimum threshold voltage, subthreshold swing, and electrical stability.⁷⁾ It is therefore desirable to search for a compromise between device electrical performance and production throughput by depositing thick a-SiN_x:H and a-

Si:H films in the shortest possible time without degrading the overall electrical characteristics of the a-Si:H TFT. One potential solution is depositing two amorphous silicon films as the active layers of the TFT: a thin layer of a low deposition rate film near the gate insulator interface in order to obtain high electronic quality a-Si:H film near the electron conduction channel, and a thick layer of high deposition rate film in the back channel to be used as the sacrificial layer during the etch back process. The a-SiN_x:H deposition is also separated into a two-step process: a thin layer of low deposition rate film near the high electronic quality a-Si:H film for optimum electrical performance and stability, and a thick layer of high deposition rate film near the gate metal to reduce gate leakage current.

The concept of double a-Si:H layer structure for TFT was first proposed by Takeuchi and Katoh for the purpose of reducing a-Si:H TFT photo-response.^{8,9)} Characteristic of dual amorphous silicon TFT was explored further by Kashiro *et al.*, and it was concluded that the field-effect mobility is highly sensitive, and linearly proportional (up to 15 nm), to the thickness of the high electronic quality a-Si:H layer.¹⁰⁾ A reduction in the thickness of the high quality film allows the defect states from the low quality film to interfere with the band bending at the a-SiN_x:H/a-Si:H interface, which causes the TFT's mobility to decrease. Tsai *et al.* investigated the effect of a low electronic quality film deposition rate on the overall electrical performance of the a-Si:H TFT.¹¹⁾ and concluded that with the increasing deposition rate the TFT's field-effect mobility decreases for the same reasoning as proposed by Kashiro. From these results it is clear that dual a-Si:H layer TFT's electrical performance can suffer due to the inclusion of the low quality film away from the a-SiN_x:H/a-Si:H interface. However, previous studies report only on the extrinsic characteristics of the a-Si:H TFT, which do not take source/drain contact resistances into consideration; yet it is well known that the presence of significant contact resistance can mask the true electrical characteristics, or the intrinsic characteristics, of an a-Si:H TFT.¹²⁾ Moreover it is not clear how the film thickness of a high quality a-Si:H affects the intrinsic and extrinsic properties of the advanced multilayer a-Si:H TFT structure. Our present work analyzes in some

*E-mail address: kanicki@eecs.umich.edu

details the advanced multilayer a-Si:H TFT with dual a-Si:H and dual a-SiN_x:H layers. We extract the electrical behaviors of the a-Si:H TFT and analyze the effect of a high quality amorphous silicon film thickness on the overall transistor performance by evaluating its intrinsic and extrinsic electrical characteristics. Based on our experimental results, we can i) quantify the effect of a high electronic quality a-Si:H thickness on the transistor's field-effect mobility, threshold voltage, subthreshold swing, and contact resistance, and ii) identify a minimum thickness of a high electronic quality a-Si:H layer required for the TFT to exhibit promising device electrical performance without unnecessarily extending the PECVD time. To our best knowledge this study is the first full analysis on the thickness effect of a high electronic quality amorphous silicon film, which include both the intrinsic and extrinsic properties of the transistor, on the dual a-Si:H and a-SiN_x:H layers transistors.

2. Experimental Methods

We fabricated back channel etched type inverted staggered transistor¹³ with patterned chromium gate (2000 Å thick) consisting of two layers of a-SiN_x:H and two layers of a-Si:H (Fig. 1): PECVD was used to deposit 3500 Å of nitrogen-rich hydrogenated a-SiN_x:H at ~1800 Å/min (G2), 500 Å of a-SiN_x:H deposited at ~1000 Å/min (G1), 100–600 Å of a-Si:H deposited at ~600 Å/min (A1), 1100–1600 Å of a-Si:H deposited at ~1200 Å/min (A2), and 700 Å of phosphorous doped amorphous silicon (n+ a-Si:H). The active island was dry-etched (SF₆ : Cl₂ : O₂ : He in 6 : 24 : 20 : 5 ratio) using a LAM 9400 TCP-RIE. Source and drain metallization includes the deposition and definition of sputtered molybdenum. Since the phosphorous from the n+ layer diffuses into the amorphous silicon film in the back channel etch TFT, it is necessary to perform dry over-etch to remove a fraction of the amorphous silicon film in order to reduce the leakage current between the source and drain;¹⁴ we dry-etched (HBr : Cl₂ in 1 : 1 ratio) 700 Å of A2 in the channel region of the transistor using the LAM 9400 TCP-RIE. All patterning steps were performed using contact photolithography via a MA-6 mask aligner. The bi-layer a-SiN_x:H surface roughness (RMS value) above the gate dielectric is about 1.1 nm. Both films have slightly different film stoichiometry, but are both N-rich (N/Si > 1.3); the Si-H content in the gate dielectric deposited at the lower rate is rather small (<0.5%). Total hydrogen content in the silicon nitride deposited at the higher rate (~36 ± 4%) is significantly larger in comparison to the film deposited at the lower rate (~28.5 ± 1.5%). The Tauc optical gap for the film deposited at higher and lower rates is about 4.6 and 5.2 eV, respectively. Table I shows the plates fabricated with different A1 and A2 a-Si:H thicknesses, denoted from here

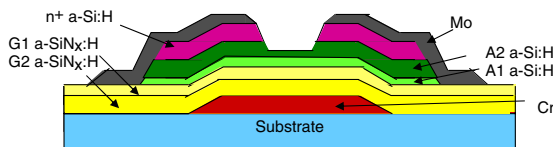


Fig. 1. (Color online) Schematic cross-section of a-Si:H TFT used in this work.

Table I. A1 and A2 a-Si:H film thicknesses of the substrates used in this study.

Plate ID	t_{A1} (Å)	t_{A2} (Å)	
		As deposited	Channel region
Var-1	100	1600	900
Var-2	200	1500	800
Var-3	300	1400	700
Var-4	400	1300	600
Var-5	500	1200	500
Var-6	600	1100	400

on as t_{A1} and t_{A2} respectively. It is important for readers to remember that the t_{A2} values presented are the deposited thicknesses, not the final A2 thicknesses in the channel region of the TFTs after the back channel etch. Electrical measurements were conducted using HP 4156 at the room temperature, and the detail of experimental techniques has been discussed elsewhere.¹³

3. Parameter Extraction Methodology

Since the goal of this study focuses on the change in a-Si:H TFT performance with respect to t_{A1} , it is imperative that we develop accurate parameter extraction techniques that represent the true TFT electrical behaviors. Changes observed, if any, should be solely due to the differences caused by electrical properties change originating from varying t_{A1} , not artificial effects contributed by the parameter extraction method. We use two different methods of extrinsic parameter extraction, which does not take contact resistance of a-Si:H TFT into consideration, to minimize the possibility of introducing artifacts: linear^{15,16} and conductance¹⁷ methods. When extracting the a-Si:H TFT parameter via the linear method, a line fits the experimental data points of the I_D-V_{GS} , or transfer, characteristic in the linear regime (Fig. 2) or the $I_D^{1/2}-V_{GS}$ characteristic in the saturation regime (Fig. 3); the data range selected is between 10–90% of the maximum drain current. The fitting line represents metal–oxide–semiconductor field-effect transistor (MOSFET) square law equations:

$$I_{D-LIN} = \frac{W}{L} C_{INS} \mu_{FE1-LIN} (V_{GS} - V_{TI-LIN}) V_{DS-LIN}, \quad (1)$$

$$I_{D-SAT}^{1/2} = \left(\frac{W}{2L} C_{INS} \mu_{FE1-SAT} \right)^{1/2} (V_{GS} - V_{TI-SAT}), \quad (2)$$

where W , L , and C_{INS} symbolize the a-Si:H TFT channel width, length, and gate insulator capacitance, respectively. Field-effect mobility values in the linear and saturation regime are denoted as $\mu_{FE1-LIN}$ and $\mu_{FE1-SAT}$; similarly threshold voltage values in each regime of operation are represented by V_{TI-LIN} and V_{TI-SAT} . The symbols V_{GS} and V_{DS-LIN} are the gate and drain biases with respect to the source terminal of the TFT. From the equations above it is clear that from the slope of the fitting line to the transfer characteristic we can extract the field-effect mobility values, and the x-intercept yields the threshold voltage.

The second method of parameter extraction is based on the conductance of the a-Si:H TFT. We begin by defining the linear regime channel conductance (σ_{CH-LIN}) of the device from the square law current equation:

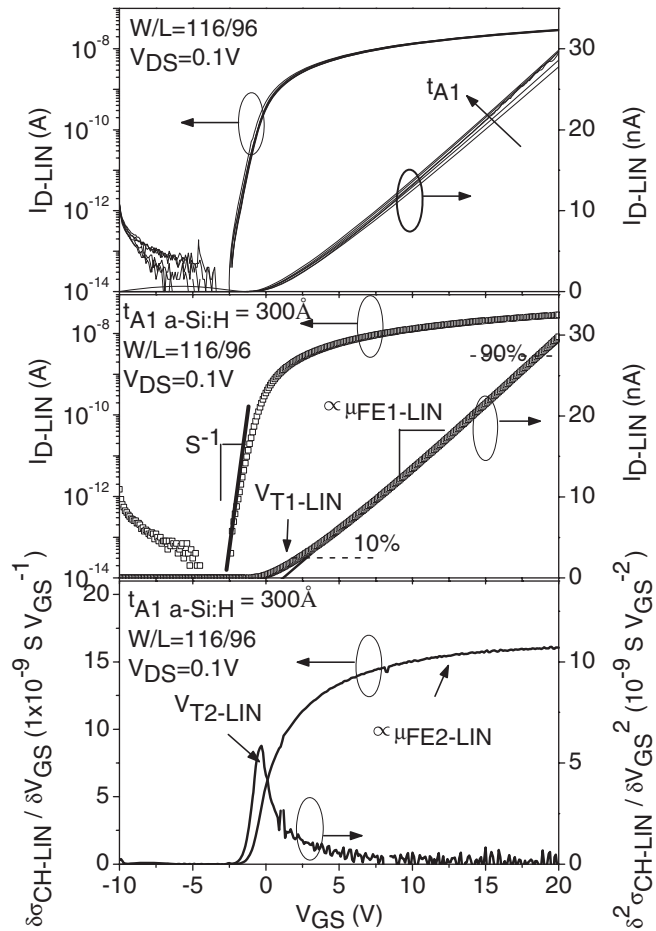


Fig. 2. Linear regime transfer characteristics of the a-Si:H TFTs with different A1 and A2 a-Si:H thicknesses (top). Experimental data points are intentionally displayed as thin lines to show the variations among different transistors. Demonstration of the parameter extraction using the linear method for TFTs with t_{A1} of 300 Å is also included: figures represent data points collected and lines represent fitting equations. Demonstration of the parameter extraction using the conductance method: calculated $\delta\sigma_{CH-LIN}/\delta V_{GS}$ and $\delta^2\sigma_{CH-LIN}/\delta V_{GS}^2$ curves for TFTs (bottom) used in this experiment.

$$I_{D-LIN} = \frac{W}{L} C_{INS} \mu_{FE2-LIN} (V_{GS} - V_{T1-LIN}) V_{DS-LIN}, \quad (3)$$

$$\sigma_{CH-LIN} \equiv \frac{\delta I_{D-LIN}}{\delta V_{DS-LIN}} = \frac{W}{L} C_{INS} \mu_{FE2-LIN} (V_{GS} - V_{T1-LIN}), \quad (4)$$

where $\mu_{FE2-LIN}$ is the linear regime field-effect mobility. To obtain the field-effect mobility we take derivative of the channel conductance with respect to the gate bias (Fig. 2):

$$\frac{\delta\sigma_{CH-LIN}}{\delta V_{GS}} = \frac{W}{L} C_{INS} \mu_{FE2-LIN}. \quad (5)$$

It should be clarified that two separate field effect mobility notations are used for the same square law equation to distinguish the difference in extraction method: $\mu_{FE1-LIN}$ in eq. (1) is a constant value with respect to V_{GS} and $\mu_{FE2-LIN}$ from eq. (5) varies with gate bias. Threshold voltage extraction from the conductance method (V_{T2-LIN}) is done by taking derivative of eq. (5) with respect to V_{GS} , and defining the maximum value as the threshold voltage. This choice is based on the fact that channel conductance changes with gate bias, as shown in Fig. 2. By defining threshold voltage as the maximum value on the $\delta^2\sigma_{CH-LIN}/\delta V_{GS}^2$ plot,

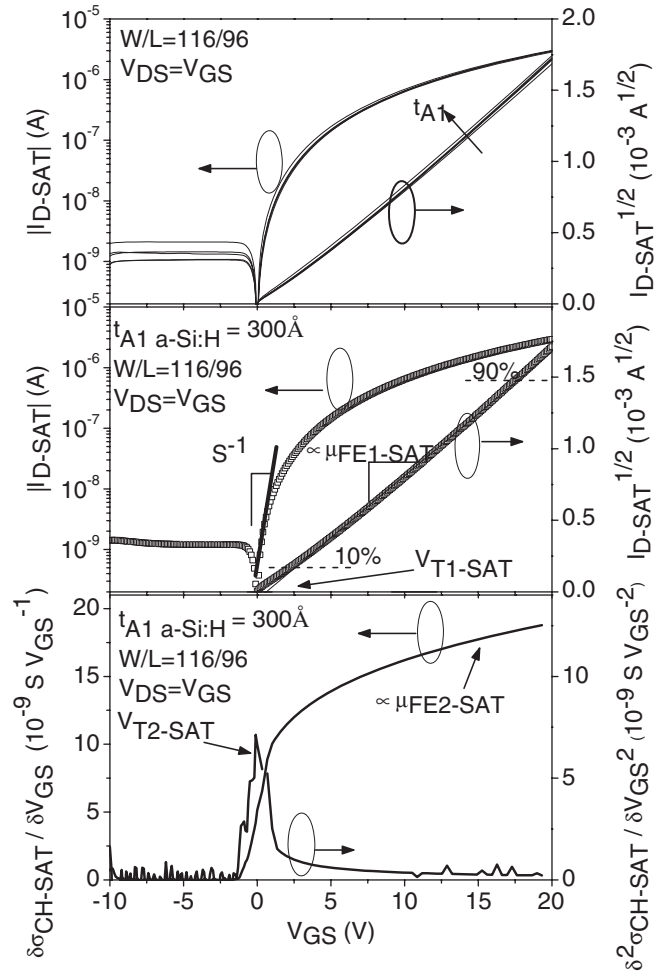


Fig. 3. Saturation regime transfer characteristics of the a-Si:H TFTs with different A1 and A2 a-Si:H thicknesses (top). Experimental data points are intentionally displayed as thin lines to show the variations among different transistors. Demonstration of the parameter extraction using the linear method for TFTs with t_{A1} of 300 Å: figures represent data points collected and lines represent fitting equations. Demonstration of the parameter extraction using the conductance method: calculated $\delta\sigma_{CH-SAT}/\delta V_{GS}$ and $\delta^2\sigma_{CH-SAT}/\delta V_{GS}^2$ curves for TFTs (bottom) used in this experiment.

we incorporate a physical origin to the threshold voltage parameter as the specific point where the maximum change in channel conductance with gate bias occurs.

Field-effect mobility extraction in the saturation regime ($\mu_{FE2-SAT}$) also begins with the square law current equation:

$$I_{D-SAT} = \frac{W}{2L} C_{INS} \mu_{FE2-SAT} (V_{GS} - V_{T1-SAT})^2. \quad (6)$$

Since $V_{DS-SAT} = V_{GS} - V_{T1-SAT}$ and $dV_{DS-SAT} = dV_{GS}$, the channel conductance in the saturation regime is

$$\sigma_{CH-SAT} \equiv \frac{\delta I_{D-SAT}}{\delta V_{DS-SAT}} = \frac{W}{L} C_{INS} \mu_{FE2-SAT} (V_{GS} - V_{T1-SAT}), \quad (7)$$

and the change in channel conductance with respect to the gate bias is

$$\frac{\delta\sigma_{CH-SAT}}{\delta V_{GS}} = \frac{W}{L} C_{INS} \mu_{FE2-SAT}. \quad (8)$$

Figure 3 shows the extractions of field-effect mobility from the $\delta\sigma_{CH-SAT}/\delta V_{GS}$ plot and threshold voltage (V_{T2-SAT}) from

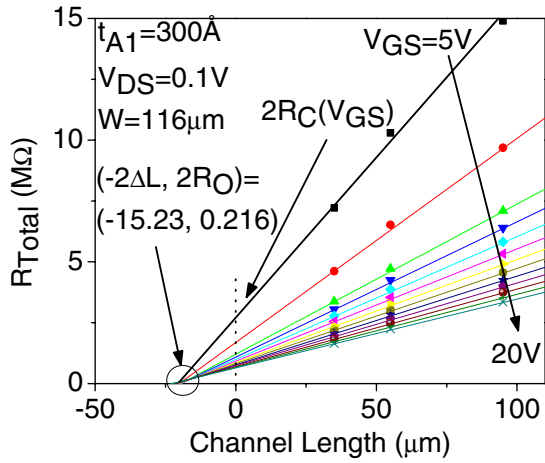


Fig. 4. (Color online) Example of the R_{TOTAL} , r_{CH} , $R_C(V_{GS})$, R_0 , and ΔL values extraction using TLM.

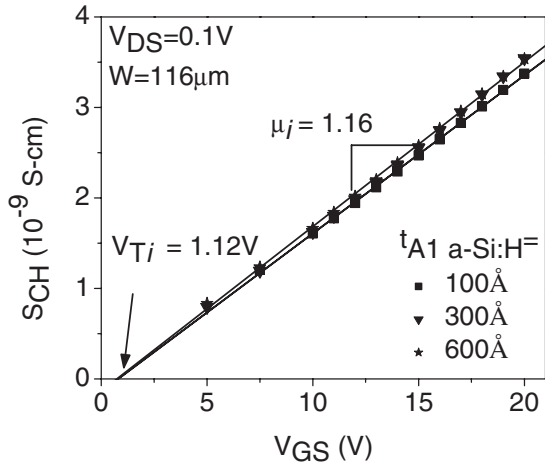


Fig. 5. Extraction of a-Si:H TFTs ($t_{A1} = 100, 300, 600 \text{ \AA}$) intrinsic mobility and threshold voltage by using channel conductivity versus gate voltage plot: symbols and lines represent experimental data and the best-fit line, respectively. Values of intrinsic mobility and threshold voltage shown belong to TFT with t_{A1} of 600 \AA .

the $\delta^2\sigma_{CH-SAT}/\delta V_{GS}^2$ plot. Both $\mu_{FE2-LIN}$ and $\mu_{FE2-SAT}$ values are extracted from the conductance curves at the maximum conductance value; in both cases maximum values occur at $V_{GS} = 20 \text{ V}$. Subthreshold swings for the linear and saturation regimes of operation are defined as the inverse values of the steepest slopes of the respective I_D-V_{GS} semi-log plots.

For the intrinsic parameter extraction, we use the transmission line method (TLM) described by Kanicki *et al.*¹⁸⁾ Detail description of the method will not be repeated here; instead we show examples of the data obtained by utilizing TLM in Figs. 4 and 5, plus the equation for total resistance (R_T) of a-Si:H TFT during the linear regime of operation:¹⁸⁾

$$\begin{aligned} R_T &= \frac{V_{DS}}{I_D} \\ &= r_{CH}(V_{GS})L + 2R_C(V_{GS}) \\ &= \frac{L}{W\mu_i C_{INS}(V_{GS} - V_{T-i})} + 2R_C(V_{GS}). \end{aligned} \quad (9)$$

In eq. (9) $r_{CH}(V_{GS})$, $R_C(V_{GS})$, μ_i , and V_{T-i} represent the channel resistivity, total contact resistance, intrinsic mobi-

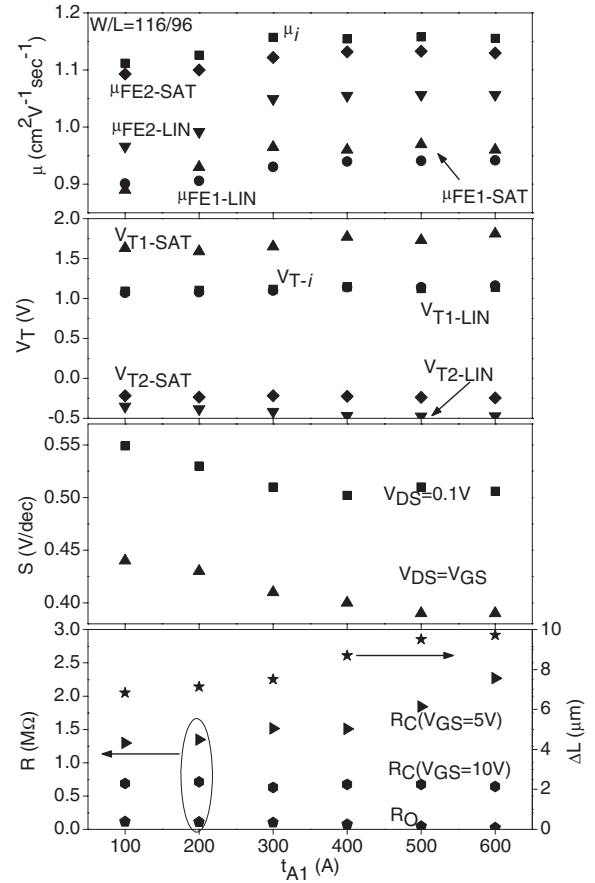


Fig. 6. Intrinsic mobility and threshold voltage, and linear and saturation regimes field-effect mobility, threshold voltage, subthreshold swing, contact resistances, and channel length deviation values for a-Si:H TFTs with different Al thicknesses investigated in this work.

lity, and intrinsic threshold voltage, respectively. From Fig. 4, we can obtain the values of $r_{CH}(V_{GS})$ and $R_C(V_{GS})$ for a given gate voltage from the slope and the y-intercept, respectively, of a fitted line for the total resistances of the transistors with different channel lengths. The minimum contact resistance (R_0) and the effective channel length change (ΔL) are extracted from the intersection of all the R_T fitted lines. Channel conductivity, $S_{CH}(V_{GS})$, is equal to the inverse value of the channel resistivity. One point worth noting is that due to the geometry of the TFT near its source and drain contacts, the actual transistor channel length is not the masked channel length L , but $L + \Delta L$. From plotting the channel conductance values with respect to the gate bias, and performing a linear fit to the data points, we can extract the intrinsic mobility and threshold voltage values respectively from the slope and the x-intercept of the best-fit line (Fig. 5).

4. Results and Discussion

From the linear regime transfer characteristics of the a-Si:H TFTs shown in Fig. 2 (top), there is a slight increase in drain current with t_{A1} . The same trend can be seen from the saturation regime transfer characteristics from Fig. 3 (top). Changes in extrinsic threshold voltage and subthreshold swing, however, are inconspicuous from observing the $I-V$ characteristics. Figure 4 shows the values of $R_C(V_{GS})$, R_0 , $S_{CH}(V_{GS})$, and ΔL of the a-Si:H TFT with $t_{A1} 300 \text{ \AA}$. Both

channel resistivity and contact resistance values decrease as V_{GS} increases. Figure 5 shows the channel conductivity plots and the values of the intrinsic mobility and threshold voltage for the TFTs with t_{A1} of 100, 300, and 600 Å. Summary of the results for the TFT extrinsic and intrinsic extractions are shown in Fig. 6.

We can make five important observation regarding the influence of amorphous silicon thickness on the performance of the TFT: i) both linear and saturation regime field-effect mobility values increase linearly by 5–9%, depending on the extraction method, when t_{A1} increases from 100 to 300 Å, and remains the same beyond that thickness, ii) a-Si:H thickness has a different effect on the threshold voltage, which depends on the extraction method, iii) subthreshold swing decreases with the increasing t_{A1} , iv) the contact resistance does change with t_{A1} , but such change depends on the applied gate bias, and v) ΔL increases from 6.5 to 10 μm with the increasing t_{A1} .

Firstly we address the 5–9% increase in the field-effect mobility. The increase is observed repeatedly and falls within the standard deviation value of our measurement (2%). This means that as t_{A1} increases from 100 to 600 Å, the short range order of the amorphous silicon film increases, and the width of the band-tail states along the electron conduction channel of the transistor decreases.³⁾ The effect of this trend has been studied in single layer a-Si:H TFTs; there is a lowering in field-effect mobility with the increasing film deposition rate caused by the increasing formation of the Si–H₂ bonds versus the ideal Si–H or Si–Si tetrahedral a-Si:H bonds.¹⁹⁾ Non-ideal bondings, such as the Si–H₂ bonds or a large concentration of Si–H bonds, distort the short range order of the amorphous silicon lattice (e.g., disorder is enhanced), thus leading to a lower field-effect mobility. We expect our A1 film to have a slightly higher density and lower content of the Si:H bonds, or a lower total hydrogen content than the A2 film because of its lower deposition rate; the Tauc gap for the A1 a-Si:H film is about 1.8 ± 0.1 eV. Also the film stress of the A1 a-Si:H film is lower in comparison to the A2 a-Si:H film, promoting better short range ordering near the interface. Indeed, according to the FTIR peak of the Si–H bond, the full-width at half-maximum (FWHM) values are ~ 94 and ~ 98 cm^{-1} for the A1 and A2 films, respectively. The Urbach edge value for such film is about 90 ± 10 meV. This explains the improvement in field-effect mobility that is associated with the increasing t_{A1} . Moreover, the increase saturates at about 300 Å, which suggests that the electron conduction is confined within that thickness because further increase in t_{A1} does not lead to higher TFT field-effect mobility; this is consistent with the channel thickness value reported previously for single layer a-Si:H TFTs.

The values and trend of the threshold voltage change with respect to t_{A1} varies with different extraction methods. Using the linear method, the extrinsic threshold voltage increases by 0.08 V as t_{A1} increase from 100 to 600 Å; the same percentage of increase can be observed in the intrinsic voltage extraction. However, when using the conductance method, there is a decrease in the threshold voltage by 0.12 V. More importantly these slight changes are close to the standard deviation value (0.1 V) of three measurements. Therefore, based on our observation we conclude that the

threshold voltage remains about the same with change in t_{A1} .

Subthreshold swing values, in both regimes of operation, decrease by 10% with increasing t_{A1} ; the decrease, however, saturates between 300 to 500 Å. Since S is a function of both a-Si:H bulk states and a-SiN_x:H/a-Si:H interface states, and we assume that TFT with different t_{A1} values have identical interface states density (N_{ss}), the lowering of S with the increasing t_{A1} originates from a decrease in neutrally charged deep-gap state density (N_{bs}) in the amorphous silicon bulk.²⁰⁾ From the subthreshold equation derived by Rolland *et al.*,²¹⁾

$$S = \frac{kT_{MEAS}}{q \log(e)} \left[1 + \frac{qX_i}{\epsilon_i} (\sqrt{\epsilon_s N_{bs}} + qN_{ss}) \right], \quad (10)$$

and assuming a constant interface state density for all a-Si:H TFTs, we can calculate the decrease in effective bulk state density from the decrease in subthreshold swing values with t_{A1} . Based on the measured S values in the linear regime for TFTs with different t_{A1} , for N_{ss} of $1 \times 10^{11} \text{ cm}^{-2} \text{ eV}^{-1}$, the effective N_{bs} changes from 9.5 to $7.7 \times 10^{18} \text{ cm}^{-3} \text{ eV}^{-1}$, while using the saturation regime S values, N_{bs} decreases from 5.7 to $4.3 \times 10^{18} \text{ cm}^{-3} \text{ eV}^{-1}$; for N_{ss} of $1 \times 10^{12} \text{ cm}^{-2} \text{ eV}^{-1}$, the N_{bs} changes from 9.3 to $7.5 \times 10^{18} \text{ cm}^{-3} \text{ eV}^{-1}$ for the linear regime and 5.6 to $4.2 \times 10^{18} \text{ cm}^{-3} \text{ eV}^{-1}$ for the saturation regime S values.

At a low gate voltage ($V_{GS} = 5$ V), the contact resistance increases with t_{A1} . As V_{GS} increases to 10 V, the contact resistance is invariant to t_{A1} and maintains a mean value of 0.67 M Ω . However, minimum contact resistance R_0 decreases with t_{A1} from 0.11 to 0.02 M Ω . To analyze the above observations we will discuss the change in $R_C(V_{GS})$ and R_0 based on the a-Si:H bulk and junction resistances of the TFT: contact resistance is the sum of the a-Si:H bulk resistance and the a-Si:H/n+ a-Si:H/Mo junction resistance. It is well known that an amorphous silicon deposited at a higher rate, therefore containing larger density of deep-gap states, has a higher dark conductivity than a-Si:H films deposited at a lower rate.²²⁾ This indicates that film A1 has a higher bulk resistivity than A2 due to its lower deposition rate. All the TFTs fabricated in this study have the same overall a-Si:H thickness of 1700 Å; transistors made on plate with the thinnest t_{A1} (100 Å) has the thickest t_{A2} (1600 Å), and *vice versa*. As t_{A1} increases from 100 to 600 Å, the thickness of the high resistivity film increases while the thickness of the low resistivity film decreases, resulting an increase in the overall contact resistance. The increase in $R_C(V_{GS} = 5$ V) with increasing t_{A1} suggests that bulk resistivity of the amorphous silicon film dominates at lower gate voltages ($V_{GS} < 5$ V). As the gate bias increases ($V_{GS} \geq 10$ V), the bulk resistivity diminishes due to increasing space charge region in the amorphous silicon. With decreasing contribution from the bulk resistivity, the junction resistivity begins to dominate, and $R_C(V_{GS})$ becomes invariant to the thickness of t_{A1} or t_{A2} . The origin of the decrease in R_0 is still being investigated. One possibility for such observation could be due to extraction artifact. Lastly the ΔL of the advanced transistor increases with A1 a-Si:H film thickness. This increase is a response to the contact resistance increase: since the bulk resistivity of the film goes up with t_{A1} at gate biases below 10 V, the cross-sectional area ($W \times \Delta L$) for the current flow has to increase to compensate for this change.

From the minimum contact resistance and ΔL values, we calculate the specific contact resistance of the TFT with t_{A1} of 300 Å to be $0.79 \Omega \text{ cm}^2$, which is quite close to the suggested value of $0.5 \Omega \text{ cm}^2$ provided by Kanicki *et al.*¹⁸⁾

5. Conclusions

We have fabricated and characterized the intrinsic and extrinsic electrical properties of the advanced a-Si:H TFT with the dual a-Si:H and a-SiN_x:H layers. Based on our investigation, the film thickness of the high electronic quality a-Si:H should be near 300 Å for the TFT to exhibit adequate characteristics without requiring long PECVD time. At t_{A1} of 300 Å, our TFT has a linear regime field-effect mobility of $0.94 \text{ cm}^2 \text{ V}^{-1} \text{ s}^{-1}$, threshold voltage of 1 V, subthreshold swing of 0.51 V/dec, R_0 of 0.1 MΩ, and specific contact resistance of $0.79 \Omega \text{ cm}^2$. For t_{A1} thinner than 300 Å we observe an increase in S while additional t_{A1} does not improve mobility, threshold voltage or subthreshold swing significantly.

Acknowledgement

One author (A. Kuo) would like to thank AKT America Inc. for financial support.

- 1) N. Ibaraki: *Mater. Chem. Phys.* **43** (1996) 220.
- 2) C. S. Chiang, C. Y. Chen, J. Kanicki, and K. Takechi: *Appl. Phys. Lett.* **72** (1998) 2874.
- 3) M. J. Powell: *IEEE Trans. Electron Devices* **36** (1989) 2753.
- 4) M. Ando, M. Wakagi, and T. Minemura: *Jpn. J. Appl. Phys.* **37** (1998) 3904.
- 5) K. Fukuda, N. Imai, S. Kawamura, K. Matsumura, and N. Ibaraki: *J. Non-Cryst. Solids* **198–200** (1996) 1137.
- 6) T. Nakahigashi, T. Hayashi, Y. Izumi, M. Kobayashi, H. Kuwahara, and M. Nakabayashi: *Jpn. J. Appl. Phys.* **36** (1997) 328.
- 7) Y. Kuo: *Vacuum* **51** (1998) 741.
- 8) Y. Takeuchi, Y. Katoh, Y. Uchida, W. I. Milne, and M. Matsumura: *J. Non-Cryst. Solids* **77–78** (1985) 1397.
- 9) Y. Katoh, O. Sugiura, Y. Takeuchi, and M. Matsumura: *Jpn. J. Appl. Phys.* **25** (1986) L309.
- 10) T. Kashiro, S. Kawamura, N. Imai, K. Fukuda, K. Matsumura, and N. Ibaraki: *J. Non-Cryst. Solids* **198–200** (1996) 1137.
- 11) J. Tsai, H. C. Cheng, A. Chou, F. C. Su, F. C. Luo, and H. C. Tuan: *J. Electrochem. Soc.* **144** (1997) 2929.
- 12) C.-Y. Chen and J. Kanicki: *Proc. SPIE* **3014** (1997) 70.
- 13) A. Kuo and J. Kanicki: *Dig. AM-FPD*, 2006, p. 39.
- 14) H. Tsutsu, T. Kawamura, and Y. Miyata: *Mater. Res. Soc. Symp. Proc.* **192** (1990) 379.
- 15) D. Schroder: *Semiconductor Material and Device Characterization* (Wiley, New York, 1990).
- 16) J. Liou, A. Ortiz-Conde, and F. Garcia-Sanchez: *Analysis and Design of MOSFET's* (Kluwer, Dordrecht, 1998).
- 17) H. Wong, M. White, T. Krutsick, and R. Booth: *Solid-State Electron.* **30** (1987) 953.
- 18) J. Kanicki, F. R. Libsch, J. Griffith, and R. Polastre: *J. Appl. Phys.* **69** (1991) 2339.
- 19) S. Yamamoto, J. Nakamura, and M. Migitaka: *Jpn. J. Appl. Phys.* **35** (1996) 3863.
- 20) S. Hasegawa and Y. Imai: *Philos. Mag. B* **46** (1982) 239.
- 21) A. Rolland, J. Richard, J. P. Kleider, and D. Mencaraglia: *J. Electrochem. Soc.* **140** (1993) 3679.
- 22) F. Gaspari, S. K. O'Leary, S. Zukotynski, and J. M. Perz: *J. Non-Cryst. Solids* **155** (1993) 149.